Effect of surface species on activity and selectivity of MoO_3/SiO_2 catalysts in partial oxidation of methane to formaldehyde

M.R. Smith [1], L. Zhang, S.A. Driscoll and U.S. Ozkan [2]

Department of Chemical Engineering, The Ohio State University, Columbus, OH 43210, USA

Received 4 October 1992; accepted 2 March 1993

The effect of the nature of surface species on the activity and selectivity of MoO_3/SiO_2 catalysts has been investigated for the partial oxidation of methane to formaldehyde. Characterization techniques including BET surface area, ambient and in situ Raman spectroscopy, X-ray photoelectron spectroscopy, and temperature-programmed reduction were used in conjunction with steady-state reaction studies to relate the presence of different surface species to the activity and selectivity of the catalyst. Results of these experiments indicate the presence of a highly dispersed silicomolybdic species with terminal Mo=O sites appearing at lower MoO_3 loadings. As the weight loading increases, these sites are transformed into polymolybdate species, forming more Mo–O–Mo bridging sites at the expense of Mo=O sites. At high weight loadings, crystalline MoO_3 begins to form. The abundance of the Mo=O sites is believed to affect activity and selectivity in the partial oxidation of methane to formaldehyde.

Keywords: Methane; formaldehyde; molybdenum oxide; silica; Raman spectroscopy; TPR; XPS

1. Introduction

In recent years, catalysis researchers have placed a heavy emphasis on the investigation of methane activation. In part, this interest has been fueled by the search to find a more efficient way to utilize natural gas reserves, which are composed largely of methane. A process which would convert methane to a more easily transportable liquid would allow for the use of many of the more remote natural gas reserves. Also, as stricter environmental laws are enacted, partial oxygenates, such as methanol, may see an increase in demand as fuel additives and substitutes.

MoO_3 supported on SiO_2 has been found to be a potentially active catalyst for

[1] Present address: International Paper Mobile, Alabama 36652, USA.
[2] To whom correspondence should be addressed.

the partial oxidation of methane by several research groups independently including Lunsford and co-workers [1,2], Somorjai and co-workers [3,4], Spencer and co-workers [5–8], and Moffat and co-workers [9–11]. Bare silica has also been reported to be active, with the main products being formaldehyde, CO_2 and CO [12,13] although it is not clear how much of the activity may be due to the presence of impurities in the silica support. The overall activity, however, was low, usually around 1% conversion of methane. When MoO_3 was added to the silica, however, the methane conversion was found to increase substantially, to values of 3–7% [5]. Several of the studies on methane activation over MoO_3/SiO_2 catalysts have been performed using N_2O as the oxidant [1,3,14]. While these studies have shown some success, the cost of N_2O would be prohibitively high for industrial use. To study the feasibility of using molecular oxygen as an oxidant in methane oxidation, research has been done comparing different oxygen sources. Barbaux et al. [14] used surface potential measurements to determine the nature of the oxygen species involved in methane oxidation. These measurements showed that, in the case of O_2 oxidant, methane was probably attacked by adsorbed O^- species, while with N_2O oxidant, methane reacted with O^{2-} species. Several papers published by Spencer and co-workers investigated methane oxidation using O_2 as the oxidant [5–8]. They observed HCHO selectivities of 30–89% in the 0–5% methane conversion range.

Although some extensive research into this area has been done, some questions still remain about the actual mechanism and the nature of active sites involved in the partial oxidation of methane. Liu et al. [1] investigated the partial oxidation of methane over MoO_3/SiO_2, and used EPR spectroscopy to show that the reaction was initiated by O^- ions coordinated to Mo^{VI} at the catalyst surface. These O^- ions were capable of abstracting H from CH_4 to form CH_3 radicals, which in turn, rapidly reacted with the surface to form methoxide complexes.

Supported MoO_3 is a catalyst which is widely used in many heterogeneous reaction applications. As such, much characterization work has been performed on the system. Temperature-programmed reduction (TPR) has been used to characterize MoO_3/SiO_2 catalysts in comparing preparation techniques, and to determine the specific surface area of the catalyst [15–17]. TPR can also yield information about the dispersion level of MoO_3 [15].

The MoO_3/SiO_2 system has also been well-characterized by Raman spectroscopy [18–20]. Raman spectroscopy is one of the most sensitive techniques available for detecting the surface species which may form as a result of interaction of MoO_3 with the SiO_2 support, and it has shown that surface species exist on SiO_2 supports up to loadings of about 1 at% [21]. Many of the Raman bands which may appear due to these surface species have been identified [19,20]. Another advantage of using Raman spectroscopy to characterize these catalysts is that it is also very sensitive to crystalline MoO_3, and so it is able to detect the formation of small crystals of MoO_3 which may not be detected by methods such as XRD. In our previous work, Raman data were correlated with reaction data in structural specifi-

city studies in C-4 [22] and C-1 [23] selective oxidation reactions to identify the location of specific active sites on MoO_3 catalysts. In situ laser Raman spectroscopy coupled with isotopic labeling technique was also used in these studies [24,25] for the identification of sites which are active for the insertion of oxygen into a hydrocarbon molecule.

Other methods used to characterize these catalysts include X-ray photoelectron spectroscopy (XPS) and X-ray diffraction (XRD). XPS has provided information about dispersion as well as the types of surface species forming [26]. X-ray diffraction (XRD) has been used to detect crystalline MoO_3 on MoO_3/SiO_2 samples [26], although Raman spectroscopy is more sensitive for the detection of crystalline MoO_3 than XRD, as the initial crystals are too small to be detected by the wavelength of X-rays.

Although many of these techniques have been used to characterize MoO_3/SiO_2 catalysts previously, most of the work has been done for other reaction systems, without much extension into the area of partial oxidation of methane. In the work presented here, Raman spectroscopy, XRD, TPR, and XPS have been used in conjunction with reaction studies to investigate the reaction pathway for the partial oxidation of methane over MoO_3/SiO_2 catalysts.

2. Experimental

2.1. CATALYST PREPARATION

The series of silica-supported molybdena catalysts used in these studies was prepared by wet impregnation using aqueous solutions of ammonium heptamolybdate, $(NH_4)_6Mo_7O_{24}\cdot H_2O$, and Cab-O-sil M5 fumed silica. Different weight loadings were prepared by varying the concentration of the ammonium heptamolybdate solution. The silica was placed in water and the ammonium heptamolybdate solution was added to the silica slurry with stirring. The pH of the solution was 4.5. The water volume was reduced by 2/3 using a rotary evaporator, and then the slurry was dried in an oven for 12 h. The catalyst was then calcined under O_2 at 675°C and pressed into pellets. The pellets were gently broken apart and sieved to 25–35 mesh. The MoO_3 loadings prepared were 0.5, 1.8, 3.5, 5.0 and 9.8 wt%.

2.2. CATALYST CHARACTERIZATION

BET surface area. The surface area was measured by the BET method using N_2 as the adsorbate. The measurement was performed using a Micromeritics 2100E Accusorb instrument.

X-ray diffraction. X-ray diffraction patterns were obtained using a Scintag PAD V Diffractometer in conjunction with a micro VAX computer for instrument

control and data acquisition. The diffractometer was operated at 45 kV and 20 mA, and used Cu Kα radiation ($\lambda = 1.5432$ Å).

X-ray photoelectron spectroscopy. X-ray photoelectron spectra were obtained using a Physical Electronics/Perkin Elmer model 550 ESCA/Auger spectrometer operated at 15 kV, 20 mA. The X-ray source was Mg Kα radiation (1253.6 eV). The C 1s binding energy (284.6 eV) was used as a reference.

Laser Raman spectroscopy. Raman spectra were obtained using a Spex Triplemate Raman spectrometer (Spex 1877) with a CCD (couple charged device) detector. The 514.5 nm line of a 5 W argon ion laser (Spectra Physics, 2017) was used as the excitation source. The ambient spectra were collected spinning the pellet in the laser beam with a total exposure time of 60 s at 50 mW laser power. The details of in situ Raman experiments have been presented elsewhere [24].

2.3. REACTION STUDIES

Steady-state methane oxidation. Reaction experiments were performed using a flow system which is described elsewhere [23]. The reactor consisted of a quartz tube with an i.d. of 5 mm. A quartz frit was used to hold the catalyst bed in place. The diameter of the quartz reactor was reduced to 2 mm at the exit of the catalyst bed to allow the gas stream to leave the heated area quickly in order to minimize gas-phase reaction. The catalyst bed was approximately 1 cm long, and 3 cm of quartz powder were placed upstream of the catalyst bed to act as a preheating zone for the reaction gases. The quartz reactor was inserted into a stainless steel block, and resistive heating cartridges were used in conjunction with a temperature controller to maintain the reactor temperature. All reactions were performed at 650°C and 1 atm. The total flow rate was 10.6 cm^3(STP)/min, with volume concentrations of 7.11% O_2, 67.14% CH_4, and 25.75% N_2. The total catalyst surface area used in the reactor was 38.0 m^2.

Analysis of the feed and reactor effluent streams was performed by an automated on-line gas chromatograph (Hewlett-Packard Series II) using both a flame ionization detector (FID) and a thermal conductivity detector (TCD). A Hayesep T column was used with both detectors to separate HCHO, CO_2, and CH_3OH. Detector response to HCHO was calibrated by flushing a nitrogen stream through a sealed beaker containing paraformaldehyde. In addition, a molecular sieve 5A column was used on the TCD with a four-port isolation valve to separate CH_4, N_2 and CO. The analytical scheme also allowed for the detection of H_2, if present. N_2 was included as an inert in the feed stream and used for internal calibration in GC analysis. The reactor effluent was sent through heated lines to the GC system and could also be sent to a GC/mass spectrometer (Hewlett-Packard 5890 Series II GC with 5989 A MS engine).

2.4. TEMPERATURE-PROGRAMMED REDUCTION STUDIES

Temperature-programmed reduction was performed using a system which was built in-house [27], consisting of a feed manifold, a reaction chamber, and a thermal conductivity detector. A vacuum system used in conjunction with the TPR allowed for an ultimate vacuum of 10^{-7} mbar for degassing samples prior to reduction. A quartz U-tube was used for the sample chamber, and an IBM compatible computer was used for instrument control and data acquisition. Experiments were performed on the basis of an equal amount of MoO_3, so the total weight of catalyst sample used was varied according to the weight loading to give a total amount of MoO_3 in the sample chamber of 14 mg for each reduction experiment. Catalyst samples were subjected to a pretreatment consisting of heating at a rate of 15°C/min from room temperature to 550°C under an O_2/N_2 stream (33 vol% O_2) with a total flow rate of 30 cm^3(STP)/min. The sample was held at 550°C for 1 h, and then cooled under vacuum to 200°C. TPR was then performed using a stream of 6 vol% H_2 in N_2 at a total flow rate of 60 cm^3(STP)/min, with a temperature ramp of 10°C/min from 200 to 950°C.

3. Results

3.1. CATALYST CHARACTERIZATION

The BET surface areas of the catalysts prepared for these studies are shown in table 1. In general, as the weight loading of MoO_3 increased the surface area of the catalyst decreased.

X-ray diffraction did not show any crystalline phases in the catalysts up to loading level of 5 wt% MoO_3. At 9.8 wt%, however, peaks corresponding to crystalline MoO_3 appeared. The XRD patterns of pure SiO_2, 5.0 wt% MoO_3, and 9.8 wt% MoO_3 are shown in fig. 1.

X-ray photoelectron spectroscopy (XPS) data were used to examine the extent of dispersion in the supported catalysts, as well as for the detection of any trace impurities in the SiO_2 support. The intensity ratio of Mo to Si signals (I_{Mo}/I_{Si}), has

Table 1
BET surface areas of MoO_3/SiO_2 catalysts

Sample	Surface area (m^2/g)
SiO_2	212
0.5 wt% MoO_3/SiO_2	200
1.8 wt% MoO_3/SiO_2	188
3.5 wt% MoO_3/SiO_2	190
5.0 wt% MoO_3/SiO_2	122
9.8 wt% MoO_3/SiO_2	88

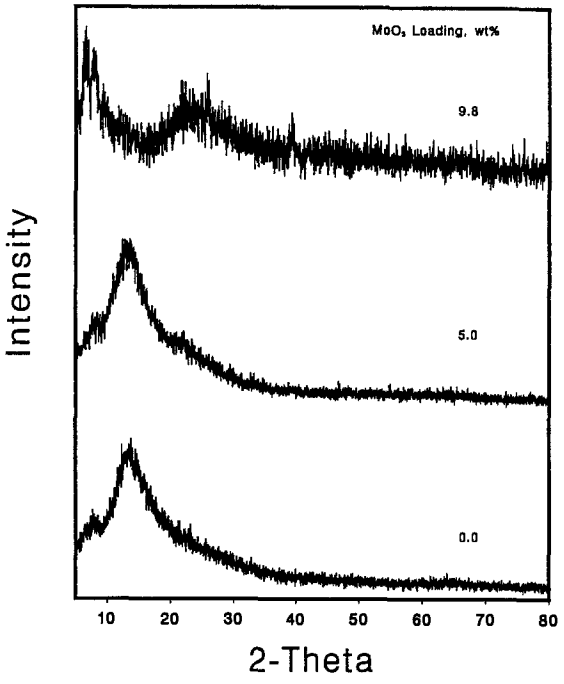

Fig. 1. X-ray diffraction patterns of SiO_2, 5.0 wt% and 9.8 wt% MoO_3/SiO_2.

been shown to be sensitive to the degree of Mo dispersion over the catalyst [26]. A plot of I_{Mo}/I_{Si} (intensity ratio of Mo $3d_{5/2}$ and Si 2p bands) versus N_{Mo}/S_{BET} (number of atoms of supported Mo per surface area) is shown in fig. 2. The curve is seen to change in slope at the higher weight loadings, indicative of the change in dispersion level. This has previously been ascribed to the progressive formation of polymolybdate at the expense of silicomolybdic species [26,28]. It should be noted that the level of dispersion of MoO_3 over SiO_2 is much lower than that over Al_2O_3

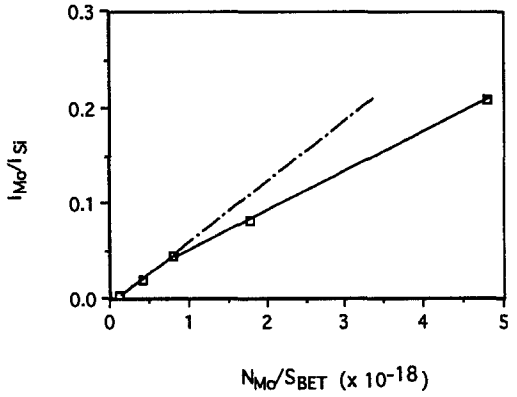

Fig. 2. XPS intensity ratio, I_{Mo}/I_{Si} versus number of Mo atoms per unit area.

[19]. The XPS spectra did not indicate the presence of any trace impurities in silica, in agreement with the technical literature provided by Cabot Corporation.

Raman spectra accumulated in the high wavenumber region (800–1000 cm^{-1}) are shown in fig. 3 for loadings of 0.0, 0.5, and 1.8 wt% MoO_3. Raman spectra for weight loadings of 3.5, 5.0, and 9.8 wt% are shown in fig. 4. These spectra were used to examine the nature of surface molybdate species on the supported catalysts. Spectra obtained at weight loadings as low as 0.5 wt% show a broad feature between 930 and 977 cm^{-1}. This band becomes even better defined at 1.8 wt% MoO_3 and could be due to a silicomolybdic species, with the band resulting from both Si–O and Mo=O stretching modes as suggested in the literature earlier [18,29,30]. Also, at 1.8 wt% loading, a weak band begins to appear between 850 and 900 cm^{-1}. This band, which is even more noticeable in the 3.5 wt% loading catalyst, has been previously attributed to the Mo–O–Mo bridging oxygen sites found in surface coordinated polymolybdate species [19]. At 5.0 wt%, there is evidence of crystalline MoO_3 appearing with bands at about 818 and 995 cm^{-1}, but there are additional bands appearing at 877, 900, 963, 977 cm^{-1}, suggesting the coexistence of crystalline MoO_3 with coordinated surface species. At 9.8 wt% loading, the

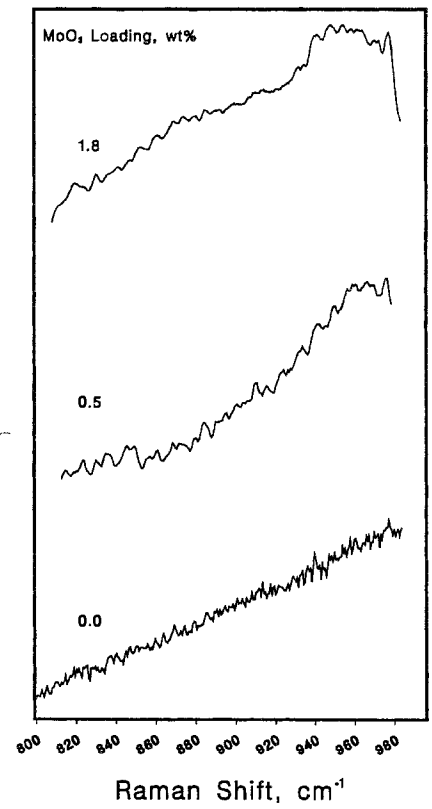

Fig. 3. Raman spectra of SiO_2, 0.5 wt% and 1.8 wt% MoO_3/SiO_2.

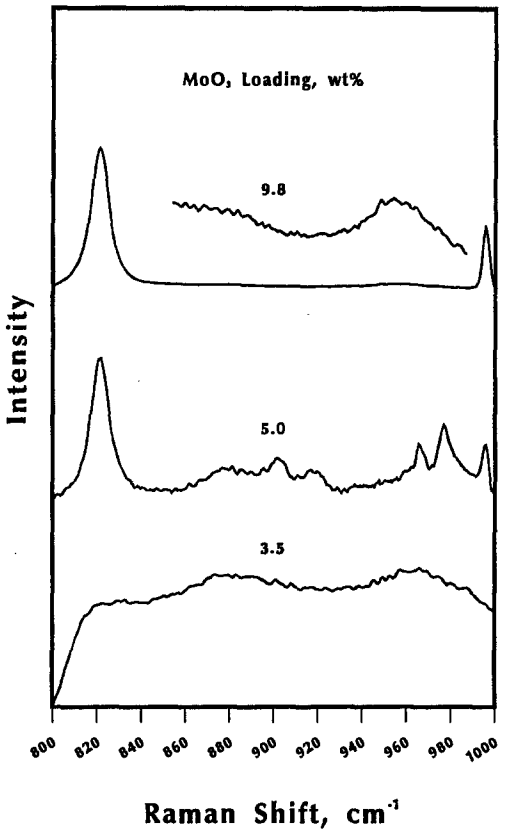

Fig. 4. Raman spectra of 3.5, 5.0, and 9.8 wt% MoO_3/SiO_2.

bands associated with crystalline MoO_3 dominate the spectrum, although the bands associated with polymolybdate species are still visible.

Fig. 5 shows a comparison of the spectra obtained over the catalyst with 5% loading at ambient conditions and after dehydration at 550°C under dry oxygen. As it is evident from the comparison of the two spectra, the dehydration process seems to change the Raman spectrum significantly. This could be due to the same "spreading phenomenon" observed earlier by de Boer et al. [20] when the molybdena/silica samples are dehydrated. The most notable change in the spectrum of the dehydrated sample is that the band at 977 cm^{-1} has become the major band. The band at 995 cm^{-1} has disappeared almost completely and the 818 cm^{-1} band has become much less intense compared to the same band observed in the hydrated sample, indicating a decrease in the abundance of crystalline molybdenum trioxide after dehydration. The relative intensity of the 960 cm^{-1} band has also decreased. Also different in this spectrum is the region in the 850–900 cm^{-1} range, showing a very weak and broad band and suggesting a decrease in the abundance of Mo–O–Mo sites although they do not seem to disappear completely. Raman spectra of

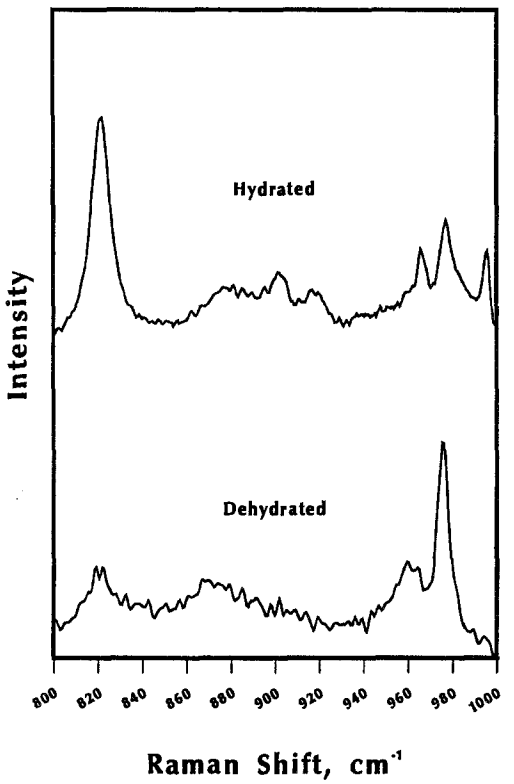

Fig. 5. Raman spectra of hydrated and dehydrated 5.0 wt% MoO_3/SiO_2.

samples with lower loading levels do not show any significant differences after dehydration.

3.2. REACTION STUDIES

Reaction runs were performed over four different catalysts: pure SiO_2, 0.5 wt%, 1.8 wt%, and 5.0 wt% MoO_3. The major products detected were HCHO, CO_2 and CO. Methanol and hydrogen were detected in trace amounts. The effect of weight loading on the rate of CH_4 conversion and on the rates of HCHO, CO_2 and CO production is shown in figs. 6 and 7, respectively. It is seen that the rate of methane conversion goes through a maximum with molybdena loading, with the maximum conversion level occurring at a weight loading of 1.8 wt%. The conversion levels vary from 2.8% for SiO_2, to 5.1% for the catalyst with 1.8 wt% loading of MoO_3. The rate of formation of HCHO is highest over the 0.5 wt% catalyst, and lowest over the 5.0 wt% sample. CO_2 rate of formation is seen to increase steadily with MoO_3 loading. The rate of CO production is highest over the 1.8 wt% catalyst, and lowest over the 5.0 wt% catalyst. Blank reactor studies performed under these conditions showed no quantifiable conversion of methane.

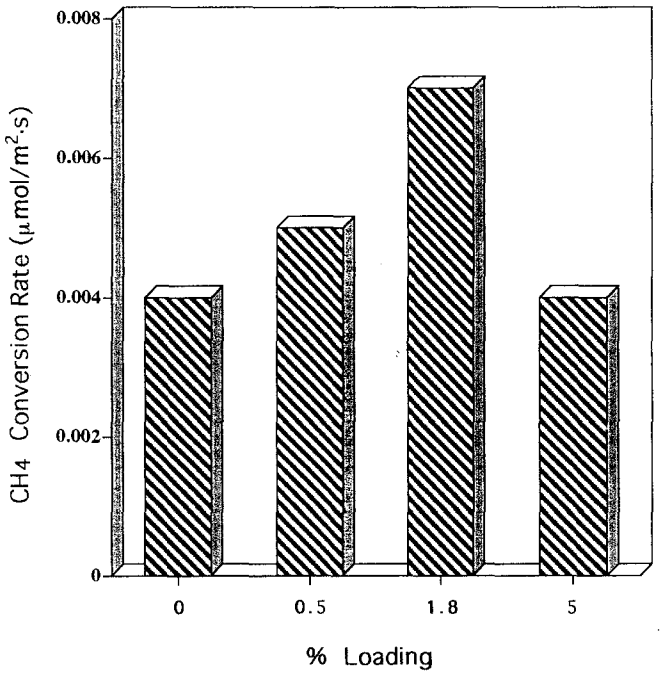

Fig. 6. Comparison of CH_4 conversion rates over SiO_2 and MoO_3/SiO_2 catalysts.

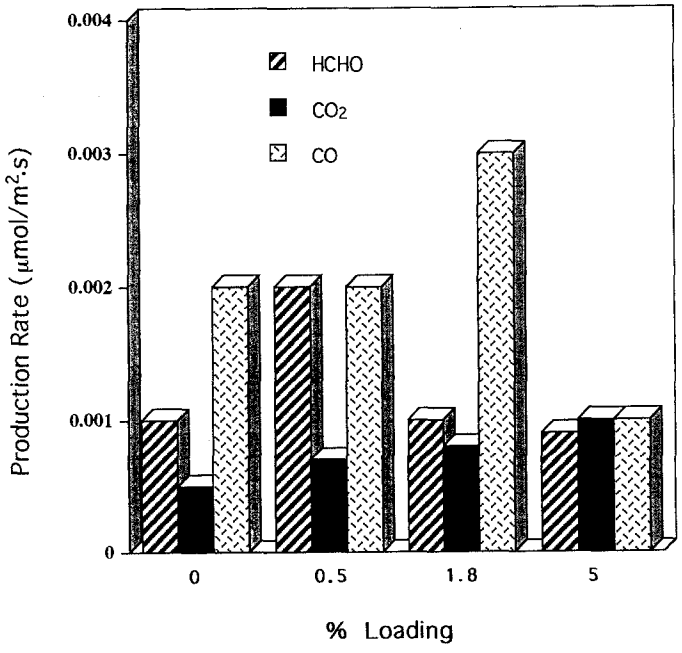

Fig. 7. Comparison of HCHO, CO and CO_2 production rates over SiO_2 and MoO_3/SiO_2 catalysts.

3.3. TEMPERATURE-PROGRAMMED REDUCTION STUDIES

Temperature-programmed reduction studies were performed over the blank SiO_2, 1.8, 3.5, 5.0 and 9.8 wt% samples. A comparison of the TPR profiles obtained over these samples is shown in fig. 8. The 0.5 wt% loading was too low to allow comparison of TPR profiles based on an equal amount of MoO_3 in the sample chamber. Blank SiO_2 did not show any reduction peaks during H_2 TPR experiments. In the TPR profile for the 1.8 wt% sample, there are three broad temperature maxima, with the dominant feature occurring at around 720°C. The other maxima are shoulder-like features at 530 and 800°C. As loading level increases to 3.5 wt%, the broad feature at 720°C disappears and two distinct temperature maxima begin to resolve at 580 and 800°C, while the shoulder peak at 530°C persists. At loading levels of 5 wt% and above, the peak around 580°C becomes very sharp, while the feature at 800°C, although better defined, still remains relatively broad. Also still visible is the shoulder peak at about 530°C.

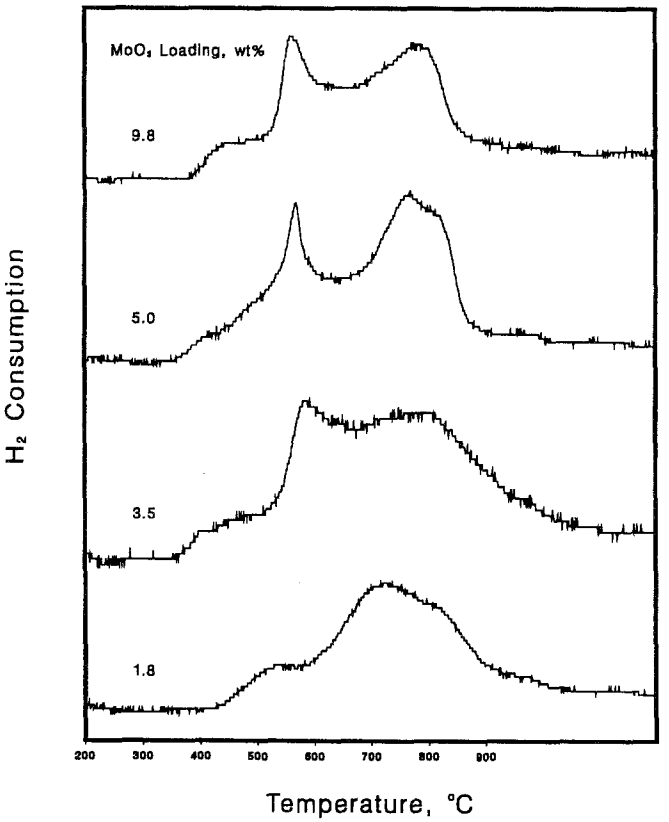

Fig. 8. TPR profiles of MoO_3/SiO_2 catalyst samples.

4. Discussion

Our characterization of SiO_2-supported MoO_3 catalysts, when combined with our reaction studies, yielded useful information on the nature of molybdena surface species active in methane oxidation. It is important to note that the silica support used in this study was free of any detectable impurities, as some of the silica supports that are commercially available do contain substantial quantities of impurities which may affect the catalytic activity and selectivity.

Our studies suggest the presence of three different species on these catalysts. At low loading levels (less than 2 wt%), the dominant structures are silicomolybdic species, as identified through Raman spectroscopy. In TPR profiles, these species are characterized by the broad maxima occurring between 650 and 800°C. As loading level increases, surface coordinated polymeric molybdate species begin to form, as evidenced by the Raman bands appearing at 880 and 960 cm^{-1}. The formation of polymeric species was also shown by the two broad TPR features appearing at 530 and 800°C. These TPR features have been attributed to polymeric molybdate surface species by other researchers as well [16]. At loading levels above 3.5 wt%, crystalline MoO_3, which is easily detected by the appearance of Raman bands at 818 and 995 cm^{-1}, begins to form. While the detection of crystalline MoO_3 at 5 wt% and above is easily achieved by Raman spectroscopy, the appearance of a rather sharp peak at 800°C in the TPR profiles is also indicative of the presence of these crystals. XPS data also show the transition from surface molybdate species to crystalline MoO_3 through the slope change of the Mo/Si intensity ratio as the number of Mo atoms/m^2 increases. Although the bands associated with crystalline MoO_3 appear to be the dominant feature in the Raman spectrum accumulated at 9.8 wt%, the bands associated with polymolybdate species are still visible, indicating the coexistence of surface and crystalline species. This coexistence is also evidenced by the appearance of broad peaks in the TPR profiles. The relatively moderate pH levels at which these catalysts were prepared can explain why larger crystals did not start forming at lower loading levels. As indicated in the literature, in highly acidic media, the dominant species in solution is $Mo_7O_{24}^{6-}$, leading to the formation of agglomerated MoO_3 precursors, which upon calcination form large MoO_3 crystals. As the solution pH increases, MoO_4^{2-} species become more dominant leading to a higher degree of dispersion for the surface species. At 9.8 wt%, the crystallites of MoO_3 formed are large enough to be detected through X-ray diffraction.

The in situ Raman spectra of the dehydrated samples gave evidence of the "spreading phenomenon" which was described in the literature earlier [20], by showing a decrease in the intensity of the bands associated with crystalline MoO_3 and polymeric molybdate species with bridging oxygen sites. However, even after dehydration, the coexistence of polymeric and silicomolybdic species at loading levels 2% and above was evident. This result is somewhat different from the findings of de Boer and co-workers [20] who observed only the isolated species at

5.6 wt% loading. However, the higher level of spreading observed in their samples could be due to the different preparation technique they used which involves deposition of Mo^{3+} ions from a solution.

Reaction studies performed over the four different weight loadings showed a strong dependence of the rates of methane conversion and product formation on the amount of molybdenum loading. The sharp decrease in the rate of methane conversion at 5.0 wt% loading corresponds to the appearance of crystalline MoO_3 in the Raman studies. This type of behavior was also reported by Spencer [6] who suggested that the crystallites of MoO_3 may be blocking the sites for methane activation.

When the turnover numbers (TON) are compared for these supported catalysts, a sharp decrease is observed as loading level changes from 0.5 to 1.8 wt%, exhibiting a 50% decrease from 0.015 to 0.007 s^{-1}. One possible explanation for this drop is the relative activity of silicomolybdic species, which are observed at low loading levels, as opposed to the relative activity of polymeric molybdate species, which begin to appear as loading level increases. It is also possible that the change in turnover number is a simple reflection of the dispersion of the catalyst over the support surface. The TON for 5.0 wt% catalyst is calculated to be around 0.004 s^{-1}.

When the comparison is extended to bulk MoO_3 using the results we have reported on structural specificity of MoO_3 in methane oxidation [23], we see that the turnover number obtained over bulk MoO_3 is comparable to the one obtained over catalysts with low loading levels, suggesting that the sites found on crystalline MoO_3 are equally capable of converting methane as those found on silica-supported catalysts. However, this comparison should be viewed cautiously as it is extremely difficult to determine a reliable value for the number of active sites exposed over bulk oxides.

The rate of formation of HCHO achieved a maximum at 0.5 wt% MoO_3. It sharply decreased at 1.8 wt%, and then decreased more slowly at 5.0 wt%. This maximum corresponds to the most dispersed sample which contains silicomolybdic species. The rate of formation of CO_2 is seen to increase steadily, while CO formation remains steady at first, then rises and falls. The highest rate of CO formation corresponds to the highest methane usage. Earlier studies performed by our group [22–25] have indicated that the terminal Mo=O site on MoO_3 was responsible for partial oxidation of hydrocarbons, while total oxidation occurred mainly on the Mo–O–Mo bridging sites. Other researchers [26] have found that the surface reaction between the anionic hydroxyl groups of the silica support and the aqueous Mo species during impregnation resulted in surface species with terminal Mo=O sites. If this is the case, as polymeric molybdate species with bridging Mo–O–Mo sites are formed at the expense of the terminal Mo=O surface species, the number of these terminal sites would decrease. This would account for the changes in the rate of formation of HCHO, as our characterization studies have indicated little, if any, polymolybdates or crystalline MoO_3 at 0.5 wt% loading. We also see that the

selectivity to CO_2 increases steadily with loading level, suggesting that complete oxidation is favored by the increased number of bridging oxygen sites. These observations are in close agreements with the results obtained in our recent studies using molybdenum oxide crystals preferentially exposing different crystal planes [23]. It also appears that the presence of silicomolybdic surface species has not promoted the further oxidation of HCHO to CO at the lowest weight loading, as the rate of formation of CO did not change between the bare support and the 0.5 wt% catalyst. The appearance of polymolybdate species seems to correlate with the sharp decrease in HCHO and the accompanying increase in CO production. Another interesting observation is that highest selectivity to CO coincides with the lowest selectivity to HCHO, suggesting that further oxidation of formaldehyde to carbon monoxide may be one of the primary steps in the reaction scheme.

Acknowledgement

The financial support for this work through National Science Foundation Grant CTS 8912247, and the partial support from AMAX Foundation are gratefully acknowledged.

References

[1] H.-F. Liu, R.-S. Liu, K.Y. Liew, R.E. Johnson and J.H. Lunsford, J. Am. Chem. Soc. 106 (1984) 4117.
[2] T.J. Yang and J.H. Lunsford, J. Catal. 103 (1987) 55.
[3] M.M. Khan and G.A. Somorjai, J. Catal. 91 (1985) 263.
[4] K.J. Zhen, M.M. Khan, C.H. Mak, K.B. Lewis and G.A. Somorjai, J. Catal. 94 (1985) 501.
[5] N.D. Spencer and C.J. Pereira, AlChE J. 33 (1987) 1808.
[6] N.D. Spencer, J. Catal. 109 (1988) 187.
[7] N.D. Spencer, C.J. Pereira and R.K. Grasselli, J. Catal. 126 (1990) 546.
[8] N.D. Spencer and C.J. Pereira, J. Catal. 116 (1989) 399.
[9] S. Kasztelan and J.B. Moffat, J. Catal. 109 (1988) 206.
[10] S. Ahmed and J.B. Moffat, Appl. Catal. 40 (1988) 101.
[11] S. Ahmed and J.B. Moffat, Catal. Lett. 1 (1988) 141.
[12] S. Kasztelan and J.B. Moffat, J. Chem. Soc. Chem. Commun. (1987) 1663.
[13] G.N. Kastanas, G.A. Tsigdinos and J. Schwank, Appl. Catal. 44 (1988) 33.
[14] Y. Barbaux, A. Elamrani and J.P. Bonnelle, Catal. Today 1 (1987) 147.
[15] R. Thomas, E.M. van Oers, V.H.J. de Beer and J.A. Moulijn, J. Catal. 84 (1983) 275.
[16] R.L. Cordero, F.J.G. Llambias and A.L. Agudo, Appl. Catal. 74 (1991) 125.
[17] J.L.G. Fierro, S. Mendioroz, J.A. Pajares and S.W. Weller, J. Catal. 65 (1980) 263.
[18] L. Rodrigo, K. Marcinkowska, A. Adnot, P.C. Roberge, S. Kaliaguine, J.M. Stencel, L.E. Makovsky and J.R. Diehl, J. Phys. Chem. 90 (1986) 2690.
[19] C.C. Williams, J.G. Ekerdt, J. Jehng, F.D. Hardcastle, A.M. Turek and I.E. Wachs, J. Phys. Chem. 95 (1991) 8781.
[20] M. de Boer, A.J. van Dillen, D.C. Koningsberger, J.W. Geus, M.A. Vuurman and I.E. Wachs, Catal. Lett. 11 (1991) 227.

[21] J.M. Stencel, *Raman Spectroscopy for Catalysis* (Van Nostrand–Reinhold, New York, 1990).
[22] R.A. Hernandez and U.S. Ozkan, I&EC Research 29 (1990) 1454.
[23] M.R. Smith and U.S. Ozkan, J. Catal. 141 (1993), in press.
[24] U.S. Ozkan, M.R. Smith and S.A. Driscoll, J. Catal. 134 (1992) 24.
[25] M.R. Smith and U.S. Ozkan, J. Catal., accepted.
[26] Y. Okamoto, T. Imanaka and S. Teranishi, J. Phys. Chem. 85 (1981) 3798.
[27] S.A. Driscoll, L. Zhang and U.S. Ozkan, in: *Catalytic Selective Oxidation*, ACS Symp. Series 523, eds. S.T. Oyama and J.W. Hightower (Am. Chem. Soc., Washington, 1993).
[28] A. Castellan, J.C.J. Bart, A. Vaghi and N. Giordano, J. Catal. 42 (1976) 162.
[29] H. Jeziorowski, H. Knözinger, P. Grange and P. Gajardo, J. Phys. Chem. 84 (1980) 1825.
[30] S. Kasztelan, E. Payen and J.B. Moffat, J. Catal. 112 (1988) 320.